

Electrochemical reactivity of aromatic compounds for use in Li cells

SHIN-ICHI TOBISHIMA, JUN-ICHI YAMAKI, AKIHIKO YAMAJI

Ibaraki Electrical Communication Laboratory, Nippon Telegraph and Telephone Public Corporation Tokai, Ibaraki-ken, 319-11, Japan

Received 15 August 1983; revised 8 January 1984

The electrochemical reactivity of aromatic compounds coupled with Li in LiClO₄-propylene carbonate was studied. Simple aromatic compounds, triphenylmethane compounds and quinone imine dyes were used. Discharge results for aromatic cathode-Li cells indicated that the relation between discharge voltage measured and reduction potential reported was approximately linear, which suggested that the discharge products were ion complexes. Also, the discharge voltage increased with an increase of their electron accepting groups and with a decrease of the electron donating strength of alkyl groups in their amino end groups. Among these compounds, rosaniline derivatives, bromo-substituted phenol red and thiazine dyes showed higher discharge voltages than 2.5 V. Methylene blue (MB) showed the largest energy density of 363 Wh kg⁻¹. Details of MB charge-discharge behavior were examined. The dynamic charge-discharge tests and cyclic voltammetry results suggested that the MB-Li cell could be cycled up to 2e per mol of MB depth. Direct reaction between the Li anode and dissolved MB seemed to be small as indicated by the Li⁺ ion conductive film formation on the Li anode.

1. Introduction

Many cathode active materials for high energy Li batteries have been studied. TiS₂, NbSe₃, V₆O₁₃ [1] and conductive polymers, such as polyacetylene [2] are typical reversible cathode active materials, based on topochemical or electrochemical doping reactions. However, few studies on aromatic cathode active materials have been reported. Quinones [3], pyrometallic dianhydride [4] and phthalocyanines [5] are rare cases of such studies.

This work reports the possible use of aromatic cathode active materials in Li cells. Simple aromatic compounds, triphenylmethane compounds and quinone imine dyes were used. Fig. 1 and Table 1 show chemical structures for these compounds. Discharge tests on these compounds coupled with Li were carried out in 1M LiClO₄-propylene carbonate. The relation between discharge voltages measured and reduction potentials reported were examined. The discharge voltage dependence on chemical structure was also investigated.

As a typical example for aromatic compounds, charge-discharge tests for methylene blue (MB) were carried out. MB was soluble in the electrolyte. Some experiments were conducted to examine the possibility of protective film formation on the Li, which avoided the self-discharge of the MB-Li cell system.

2. Experimental details

Reagent grade aromatic compounds (Tokyo Kasei Co.) as the cathode active materials were used after drying at 60° C in vacuo for several days. A laboratory type cell [5], shown in Fig. 2, was used to examine the cathode active material properties. A Li disc anode (3.14 cm²) was prepared by pressing a Li wire (c. 3 mm φ). Current density was calculated by using this anode surface area. The cathode mixtures were prepared by mixing appropriate amounts of cathode active material and acetylene black (AB, Denki Kagaku Co.). A carbon felt sheet (Nippon Carbon Co.) was used to prevent direct reaction between the cathode active material and the Li metal.

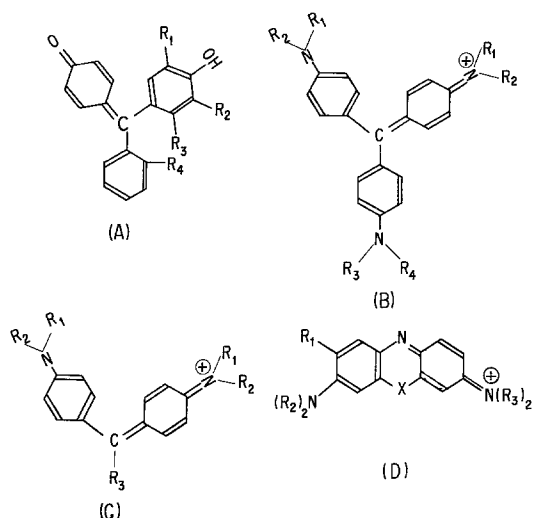


Fig. 1. Chemical structures of aromatic compounds used. (A) Triphenylmethane acid-base indicators, (B) and (C) triphenylmethane dyes, (D) quinone imine dyes.

A porous polypropylene sheet (Polyplastic Co.) was used as a separator. The electrolyte was 1M LiClO₄-distilled propylene carbonate (PC, Tokyo Kasei Co.) solution. Water content was less than 200 ppm.

The cell shown in Fig. 3 was used to examine Li-MB reactions under galvanostatic charge-discharge operation with a visual spectrometer

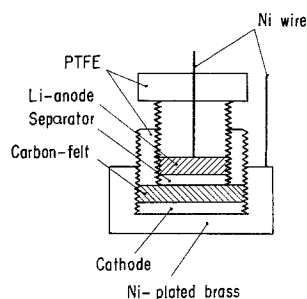


Fig. 2. Cell configuration for discharge tests of aromatic compound-Li couples. PTFE is polytetrafluoroethylene.

(Shimazu Co. Model UV-365). This cell is U-shaped to prevent mixing of the reaction products between the two electrodes. It has a Li sheet electrode and a Ni net electrode.

Capacitance and resistance of the Li electrode in LiClO₄-PC-MB solution were measured by the coulostatic method [6] to evaluate the MB solubility influence (Fig. 4). In the coulostatic technique, 0.1 μC was injected into the Li electrode from a small capacitor (0.01 μF). The resultant change of potential was converted to log *V* using an electrometer and digital recorder. The sampling interval was 2 μsec. The charge divided by the change of potential (extrapolated to zero time) then gave the electrode capacitance. The

Table 1. Structure of aromatic compounds

Structural group in Fig. 1.	Compound	R ₁	R ₂	R ₃	R ₄	X
A	phenol red	H	H	H	SO ₃ Na	
	bromothymol blue	CH(CH ₃) ₂	Br	CH ₃	SO ₃ Na	
	bromocresol green	Br	Br	CH ₃	SO ₃ Na	
	bromophenol blue	Br	Br	H	SO ₃ Na	-
	cresol red	CH ₃	H	H	SO ₃ Na	
	<i>o</i> -cresolphthalein	CH ₃	H	H	CO ₂ Na	
B	rosaniline	H	H	H	H	
	crystal violet	CH ₃	CH ₃	CH ₃	CH ₃	-
	acid brilliant blue R	C ₂ H ₅	C ₂ H ₄ SO ₃ Na	C ₂ H ₅	C ₂ H ₅	
C	brilliant green	C ₂ H ₅	C ₂ H ₅	C ₆ H ₅	-	-
	erio green B	CH ₃	CH ₃	C ₁₀ H ₅ S ₂ O ₆ *		
D	methylene blue	H	CH ₃	CH ₃		S
	neutral red	CH ₃	H	CH ₃		NH
	Capri blue	CH ₃	C ₂ H ₅	CH ₃		O
	thionine	H	H	H	-	S
	toluidine blue	CH ₃	H	CH ₃		S
	nile blue	C ₄ H ₄ *	H	C ₂ H ₅		O
	methylene green†	H	CH ₃	CH ₃		S

* Condensed benzene rings; † also have -NO in *p*-position in a ring. The structure of aurin has =O and two -OHs instead of rosanilines' three -NH groups, Groups B, C and D have Cl⁻ counter anion.

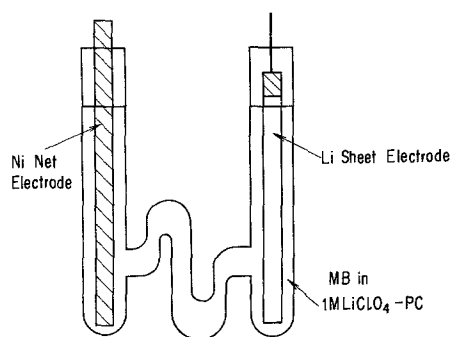


Fig. 3. Cell configuration to examine the MB-Li reaction. Li electrode (150 × 10 × 0.5 mm), Ni electrode (150 × 10 × 0.5 mm).

slope of the t - $\ln V$ plot divided by the electrode capacitance gave the electrode resistance.

Cyclic voltammetry for MB in 1M LiClO₄-PC was carried out by using a cell similar to that of Rauh *et al.* [7] with a Li disc anode (1 cm²), a Li reference electrode and a Pt working (0.32 cm²) electrode.

All the cells were constructed and tested in an argon filled dry box.

3. Results and discussion

3.1. Discharge characteristics of aromatic compounds coupled with Li

Discharge tests for Li-aromatic compound cells were carried out at a constant current of 1 mA (0.32 mA cm⁻²). Most of the discharge curves showed one flat part, which was followed by a gradually decreasing part. The potential for the

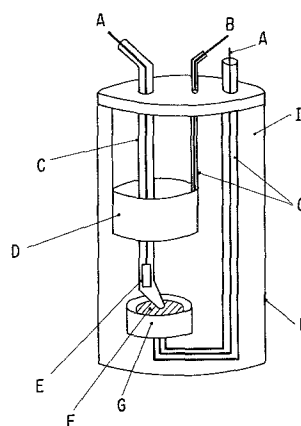


Fig. 4. Cell configuration for resistance and capacitance measurements in LiClO₄-PC added MB (4×10^{-3} M). A - Ni wire, B - Ti wire, C - glass tube, D - Li counter electrode (150 × 10 × 0.5 mm), E - Li reference electrode, F - Li working electrode (20 mm ϕ × 0.5 mm), G - PTFE holder, H - Pyrex case, I - MB-LiClO₄-PC solution.

PC-Li reaction on a graphite electrode was reported to be 0.6 V vs Li [8]. So we can not deny the possibility that the second part may correspond to a PC-Li reaction. Therefore, the voltage, capacity and energy density obtained from the first plateau was used to evaluate the cell characteristics. In the case of simple aromatic compounds consisting of only hydrogen and carbon atoms, initial discharge voltages were 1.1-1.5 V, as shown in Table 2. However, higher discharge voltage is required for a Li battery. Therefore, triphenylmethane compounds and quinone imine dyes with electron accepting groups and/or high reduction potentials were examined.

Table 2. Discharge characteristics for simple aromatic compound-Li cells at 1 mA (0.32 mA cm⁻²)*

Cathode active material	Molecular weight	Discharge [†] capacity (Ah kg ⁻¹)	Energy [†] density (Wh kg ⁻¹)	Discharge voltage (V)	Utilization [‡] (%)
anthracene	178.23	80	104	1.30	27
pyrene	202.26	74	86	1.16	28
phenanthrene	178.23	60	74	1.23	20
perylene	252.31	69	97	1.40	33
naphthalene	128.21	48	62	1.28	12
naphthacene	228.29	26	36	1.40	11
acetylene black (AB)	-	12 [§]	16 [§]	-	-

Cathode Composition: 0.05g AB + 0.05g cathode active material

* Values for the first plateau of the discharge curves; [†] values based on only cathode active material weight; [‡] values based on 2e transfer; [§] values based on AB weight only.

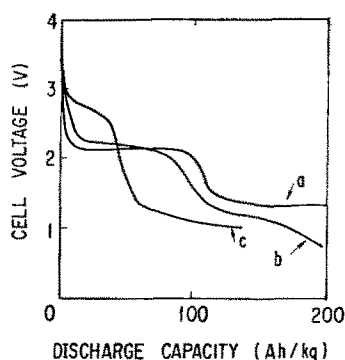


Fig. 5. Discharge curves for triphenylmethane compound-Li cells with 1M LiClO₄-PC at 1 mA: (a) crystal violet, (b) rosaniline, (c) aurin. Cathode composition, 0.05g acetylene black and 0.05g cathode active material.

3.1.1. *Triphenylmethane compounds.* Triphenylmethane compounds (TPM) used in this work were separated into two groups according to their properties, i.e. triphenylmethane acid-base indicators shown in Fig. 1A and triphenylmethane dyes shown in Fig. 1B and C. Fig. 5 shows some typical discharge curves for triphenylmethane dye-Li cells. The initial discharge voltages for TPM cells were 0.5–1.0 V higher than those for the non-substituted aromatic compound cells. Table 3 summarizes the discharge cathode characteristics for the TPM cells.

In the case of triphenylmethane acid-base indicators, the initial discharge voltages increased with increasing electron accepting groups and also

decreasing electron donating groups, as shown in Table 4. As the cell voltages, open circuit voltages (OCVs), were not used. The OCV is reported not to reflect the effective voltage for the cathode active material because OCV varied with adsorbed impurities, such as oxygen, on the cathode [9].

The dependence of the discharge voltages for triphenylmethane dyes on ($-x$) was briefly examined: ($-x$) is a parameter in the Hückel approximate equation for the lowest unoccupied molecular orbital (LUMO) energy level (E), $E = \alpha + \beta x$ [10]. The relation between ($-x$) and reduction potential is known to be linear if the solvation energy is the same [10]. Reported and calculated ($-x$) values and initial discharge voltages are shown in Table 5. Parameter ($-x$) decreased in the order $N(C_2H_5) > N(CH_3) > NH_2$ for amino end groups. The decrease in ($-x$) means an increase in cell voltage. So, rosaniline with NH_2 end groups showed a higher voltage value (2.75 V) than that for crystal violet with $N(CH_3)$ end groups. The calculated ($-x$) value for brilliant green was low. This lower ($-x$) value for brilliant green than for rosaniline could not explain the lower voltage for brilliant green. This may be caused by the rough perturbation method. In this method, the effects of $\Delta\alpha'_i$ s and $\Delta\beta'_{ij}$ s other than $\Delta\alpha_N$ are assumed to be negligible ($\Delta\alpha_i$ = the difference in the coulomb integral of the i th atom caused by the perturbation. $\Delta\alpha_N = \Delta\alpha_i$ of nitrogen atom, $\Delta\beta_{ij}$ = the

Table 3. Discharge characteristics for triphenylmethane compound-Li cells at 1 mA (0.32 mA cm⁻²)*

Cathode active material	Molecular weight	Discharge capacity [†] (Ah kg ⁻¹)	Energy density [†] (Wh kg ⁻¹)	Discharge voltage (V)	Utilization [‡] (%)
crystal violet	407.99	100	214	2.14	76
aurin	290.32	59	163	2.75	32
erio green B	560.61	40	92	2.30	42
brilliant blue R	825.99	56	152	2.70	87
rosaniline	325.67	79	217	2.75	48
brilliant green	482.64	20	46	2.30	18
phenol red	354.38	121	260	2.15	80
bromothymol blue	624.38	60	147	2.45	70
<i>o</i> -cresolphthalein	346.38	60	115	1.90	39
bromophenol blue	669.96	50	136	2.75	62
bromocresol green	698.01	38	104	2.72	50
cresol red	382.43	24	43	1.80	17

Cathode Composition: 0.05g AB + 0.05g cathode active material.

* Values for the first plateau of the discharge curves; [†] values based on only cathode active material weight, [‡] values based on 2e transfer.

Table 4. Relation between initial discharge voltage and functional groups in triphenylmethane acid-base indicators

Cathode active material	Initial discharge voltage (V)	Functional groups	
		Electron donating	Electron accepting
bromophenol blue	2.75	—	— Br × 2
bromocresol green	2.72	— CH ₃	— Br × 2
bromothymol blue	2.45	— CH ₃ , — CH(CH ₃) ₂	— Br
phenol red	2.15	—	—
<i>o</i> -cresolphthalein	1.90	— CH ₃	—
cresol red	1.80	— CH ₃	—

difference in the resonance integral of the *i*th atom and *j*th atom caused by perturbation).

Rosaniline type compounds in Fig. 1B showed relatively larger energy density. For example, crystal violet showed 214Wh kg⁻¹. Otherwise, triphenylmethane acid-base indicators showed relatively smaller energy density, which may be due to the Na⁺ and H⁺ influence in their composition.

3.1.2. *Quinone imine Dyes*. Fig. 6 shows discharge curves for quinone imine dye (QID)-Li cells. The initial discharge voltages for QID cells were relatively higher. For example, methylene blue (MB) showed approximately 1.2 V higher a voltage than that for the perylene cell, which showed the highest voltage among the simple aromatic compounds. This voltage difference between MB and perylene was about the same as the reported reduction potential difference in dimethylformamide [12]. Table 6 summarizes the discharge cathode characteristics for QID cells.

Fig. 7 shows the relation between the initial discharge voltages measured and redox potentials

Table 5. Relation between LUMO energy and discharge voltage of some triphenylmethane compounds

Compound	Initial voltage (V)	(-x)*
Döbner's violet	—	0.320 [†]
brilliant green	2.30	0.408 [‡]
rosaniline	2.75	0.414 [†]
crystal violet	2.14	0.494 [‡]

*(-x) means LUMO energy level parameter by Hückel approximated equation for LUMO energy level (*E*), $E = \alpha + \beta x$ [10]; [†] reported values [11]; [‡] (-x) values were calculated by perturbation theory based on (-x) reported for Döbner's violet and rosaniline [11].

reported for QID [13]. The relation was linear. Compared with MB and thionine, the voltages increased with decreasing the electron donating strength of the alkyl groups in their amino end groups, as in the case of triphenylmethane compounds. For the hetero atom effects in the centre of the QID rings, cell voltages decreased in the order of thiazine with N and S atoms > oxisazine with N and O atoms > azines with N and N atoms. These tendencies were also predicted by the Linear Combination of Atomic Orbital (LCAO) Molecular Orbital (MO) theory (see Appendix).

MB showed a discharge capacity of 141 Ah kg⁻¹, corresponding to the plateau of the discharge curve. This capacity was equal to 1.7*e* transfer per mol of MB, based on the Faraday constant and MB molecular weight. As a typical example for aromatic compounds, charge-discharge characteristics and reaction mechanism for MB were examined.

3.2. Charge-discharge characteristics of MB

A charge-discharge test for the MB-Li cell was

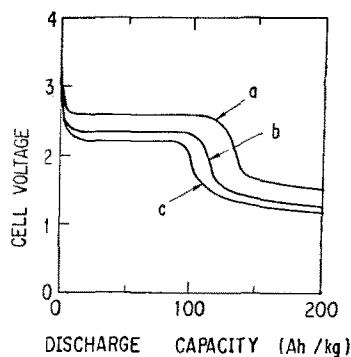


Fig. 6. Discharge curves for quinone imine dye-Li cells at 1 mA: (a) methylene blue, (b) neutral red, (c) Capri blue.

Table 6. Discharge characteristics for quinone imine dye-Li cells at 1 mA (0.32 mA cm^{-2})^{*}

Cathode active material	Molecular weight	Discharge [†] capacity (Ah kg^{-1})	Energy [†] density (Wh kg^{-1})	Discharge voltage (V)	Utilization [‡] (%)
methylene blue	319.85	141	363	2.58	84
neutral red	288.78	121	282	2.34	65
Capri blue	345.87	120	263	2.20	77
thionine	263.74	100	263	2.63	49
methylene green	364.85	104	265	2.54	71
toluidine blue	305.82	117	302	2.57	67
Nile blue	353.85	100	245	2.45	66

Cathode Composition: 0.05g AB + 0.05g cathode active material.

^{*} Values for the first plateau of the discharge curves; [†] values on only cathode active material weight; [‡] values based on $2e$ transfer.

carried out galvanostatically at 1 mA under a constant charge-discharge capacity of 100 Ah kg^{-1} ($1.2e$ per mol of MB). Fig. 8 shows charge-discharge curves for an MB-Li cell. Numbers in Fig. 8 are charge-discharge cycle numbers. The MB-Li cell was found to be rechargeable for about 20 times.

3.3. Reaction mechanism of MB

The change of MB with charge-discharge operation was examined by visual spectrometry. The results are shown in Fig. 9. As shown in Curves a and b in Fig. 9, MB absorbance ($\lambda_{\text{max}} = 630 \text{ nm}$; blue) at an Ni net cathode decreased with discharge and the solution turned slightly yellow. This λ_{max} was considered to be in the UV region. With the following charge, this colourless solution turned blue again, as shown in Curve c in Fig. 9.

MB absorbance at the Li electrode did not change during the process. These results indicate that the MB-Li electrochemical reaction is reversible. MB was chemically reacted with $n\text{-C}_4\text{H}_9\text{Li}$ in the presence of PC. The products were slightly yellow species. By H_2O addition to this solution, it turned blue again. This result also suggests that the MB-Li reaction is reversible. In addition, cyclic voltammetry for MB was carried out. As shown in Fig. 10, the results indicate a two-step reversible redox reaction for MB. The redox potentials were 2.85 and 2.6 V, respectively (these values were lower than those reported in aqueous solution [12]). The species formed by the first reduction of MB seems to be unstable because corresponding peaks are smaller than others. For this reason, the discharge voltage did not show the two-step profile up to $1.7e$ mol of MB depth. The initial discharge voltage was 2.6 V, which value showed good agreement with the

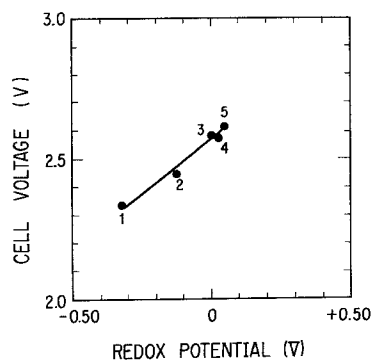


Fig. 7. Relation between initial discharge voltages and redox potential [13] for QID: 1. neutral red, 2. Nile blue, 3. Methylene blue, 4. toluidine blue, 5. thionine.

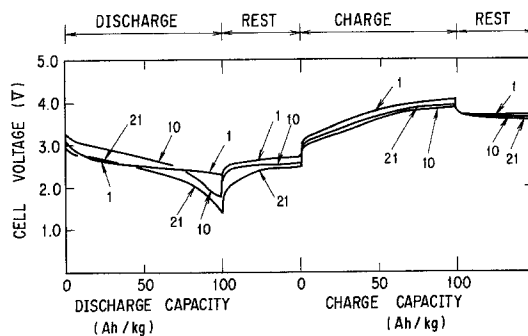


Fig. 8. Charge-discharge curves for MB-Li cell at 100 Ah kg^{-1} capacity. Cathode composition: 0.01 g acetylene black and 0.01g MB. Rest time 30 min.

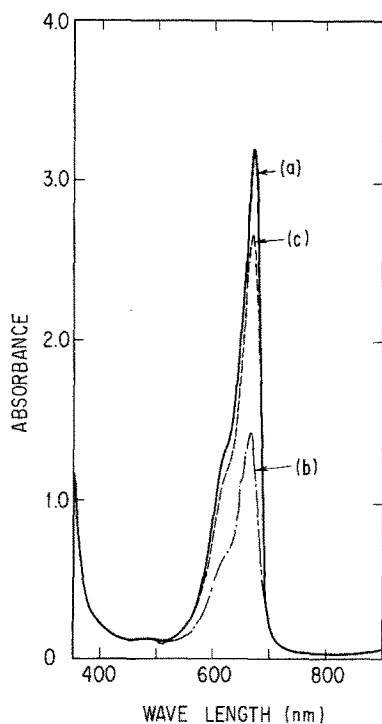


Fig. 9. Visual spectrum for MB coupled with Li under charge-discharge operation in 1M LiClO₄-PC (MB in 8×10^{-4} M): (a) 0.38 mA h discharge, (b) 6.0 mA h discharge, (c) 0.25 mA h charge.

second reduction potential measured by cyclic voltammetry. We believe MB could be cycled up to a $2e$ transfer per mol of MB depth. Furthermore, the H-MB reaction is reported [12, 14] to be a $2e$ reversible reaction. If we can assume the similarity of the reactivity between H and Li, the MB-Li reaction is also a $2e$ transfer reversible reaction.

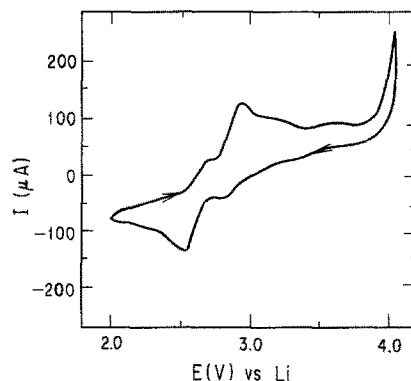


Fig. 10. Cyclic voltammogram for MB coupled with Li in the Li-Pt cell with 1M LiClO₄-PC (MB in 8×10^{-4} M); scan speed 10 mV s^{-1} .

3.4. MB solubility influence on cathode characteristics

Although MB is soluble at $c. 5 \times 10^{-2} \text{ mol l}^{-1}$ in PC, MB can be discharged and can even be charged. To explain these phenomena, the capacitance (C) and resistance (R) on Li in LiClO₄-PC-MB were measured. The results are shown in Figs. 11-13, corresponding to R and C of Li for simple standing after discharge and after charge, respectively. The data shown are average values for five repeated measurements and the points combined with the broken lines correspond to before and after the charge or the discharge. In the MB added solution, for example, R initially decreased and gradually increased by simple standing. R was almost constant with discharge. Otherwise, in LiClO₄-PC alone, R changes differed, i.e. R increased with simple

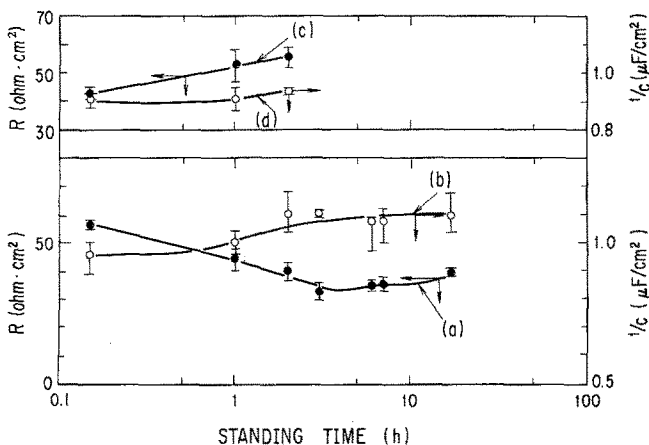


Fig. 11. Resistance and capacitance for Li anode by Li standing. (a) and (b) in 1M LiClO₄-PC added MB (4×10^{-3} M), (c) and (d) in 1M LiClO₄-PC alone.

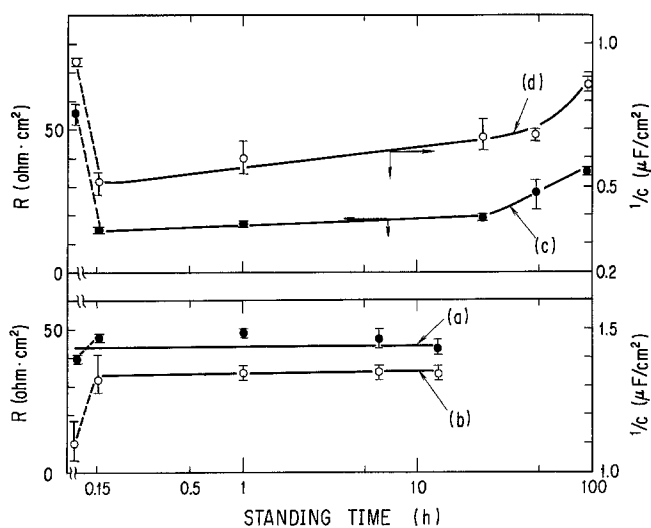


Fig. 12. Resistance and capacitance for Li by discharging, (a) and (b) in 1M LiClO₄-PC added MB (4×10^{-3} M), (c) and (d) in 1M LiClO₄-PC alone.

standing and R decreased with discharge. These results suggest that an Li⁺ ion conductive film is formed on the Li in MB added solution. Such a protective film is reported in the cases of SOCl₂ [15] and SO₂ [16]. A similar interpretation for a Li surface was reported using a similar method in the cases of SOCl₂ [15] and SO₂ [16]. Furthermore, this film was broken by charge, as shown in Fig. 13. Although this Li⁺ ion conductive film composition is not clear, LiCl [17] or MB-Li may be possible. The self-discharge for this cell system may be so small because of the protective film formation on the Li surface.

4. Conclusion

The electrochemical reactivity of aromatic com-

pounds coupled with Li and the possibility of the use of aromatic cathode active materials for nonaqueous Li batteries were examined. By the discharge tests, the discharge voltages were found to depend on the ease of reduction, which was expected from chemical structure, functional groups, reduction potential and LUMO energy levels. The relation between reduction potential and discharge voltage was linear, which suggested that discharge products were ion complexes. Rosaniline derivatives, bromo-substituted phenol red and thiazine compounds showed relatively higher voltages than 2.5 V. For the energy density, MB showed the highest value of 363 Wh kg⁻¹. Cycle life for the MB-Li cell was about 20 times at 100 Ah kg⁻¹ (1.2 e per mol of MB) depth. We believe MB reacts with Li reversibly up to 2e

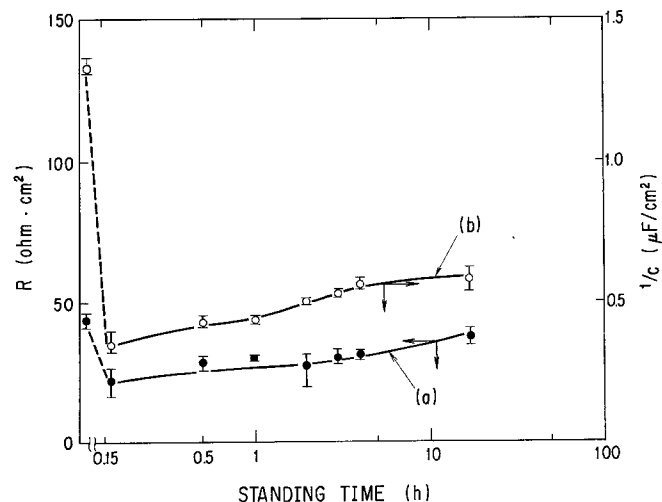


Fig. 13. Resistance and capacitance for Li by charging in 1M LiClO₄-PC added MB (4×10^{-3} M).

per MB depth from the results of cyclic voltammetry. Though MB was soluble in the electrolyte, MB could be discharged and could even be cycled. This was found to be due to a Li^+ ion conductive film formation on the Li. So it is believed that aromatic compounds are prospective practically useful cathode active materials for Li batteries.

Acknowledgement

The authors would like to express their gratitude to Mr C. Uemura, Mr T. Inamura and Mr T. Okada for their helpful guidance and discussion during the course of this research.

Appendix

LUMO energy level of QID

A crude estimate for $(-x)$ of QID based on the method reported by Itoh [11] was tried. The results are, methylene blue $-(x) = 0.0651$, $\delta_N = 0.4$, $\delta_{CN} = \delta_N/8$, $\delta_{RN} = 1.30$, $\delta_{CNR} = \delta_{RN}/8$, S atom (Longues-Higgins see Streitwieser, Jr. [18]); thionine $-(x) = 0.00958$, perturbation treatment $\Delta\delta_{RN} = 0.3$; toluidine blue $-(x) = 0.0637$, perturbation treatment $\Delta\delta_{R_2N} = 0.3$, $\Delta\delta_{C-CH_3} = -0.5$; capari blue $-(x) = 0.124$, $\delta_0 = 2$, $\delta_N = 0.4$, $\delta_{CN} = \delta_N/8$, $\delta_{RN} = 1.0$, $\delta_{CNR} = \delta_{RN}/8$, perturbation treatment, $\Delta\delta_{R_2N} = 0.4$, $\Delta\delta_{R_3N} = 0.3$, $\delta_{C-CH_3} = -0.5$

where the coulomb integral was defined by $\alpha_x = \alpha_0 + \delta_x\beta_0$.

References

- [1] B. Scrosati, *Electrochim. Acta.* **26** (1982) 1559.
- [2] P. J. Nigrey, D. Macinnes, Jr., D. P. Nairns and A. G. MacDiarmid, *J. Electrochem. Soc.* **128** (1981) 1651.
- [3] H. Alt, H. Binder, A. Khling and G. Sundstede, *Electrochim. Acta.* **17** (1972) 873.
- [4] T. Ohzuku, H. Wakamatsu, Z. Takehara and S. Yoshizawa, *ibid.* **24** (1977) 723.
- [5] J. Yamaki and A. Yamaji, *J. Electrochem. Soc.* **129** (1982) 5.
- [6] E. Yeager and A. J. Salkind (Eds.) *Techniques of Electrochemistry*. Vol. 1, Wiley Interscience, New York (1972) p. 97.
- [7] R. D. Rauh, T. F. Reise and S. B. Brummer, *J. Electrochem. Soc.* **125** (1978) 186.
- [8] A. N. Dey and B. P. Sullivan, *ibid.* **117** (1970) 222.
- [9] C. Iwakura, N. Isobe and H. Tamura, *Electrochim. Acta.* **28** (1983) 277.
- [10] A. Streitwieser, Jr., 'Molecular Orbital Theory for Organic Chemists', Chap. 7, John Wiley & Sons, Inc., New York (1961).
- [11] R. Itoh, *J. Phys. Soc. Jpn.* **12** (1957) 644.
- [12] L. Meites and P. Zuman, 'CRC Hand Book Series in Organic Electrochemistry. Vol. 1', CRC Press Inc., Ohio (1977) pp. 692, 768.
- [13] M. Koizumi, H. Obata and S. Hayashi, *Bull. Chem. Soc. Jpn.* **37** (1964) 108.
- [14] H. Obata, *ibid.* **34** (1961) 1057.
- [15] R. V. Moshkev, Y. Geronov and B. Puresheva, *J. Electrochem. Soc.* **128** (1981) 1851.
- [16] R. V. Moshkev and Y. Geronov, *J. Power Sources* **8** (1982) 395.
- [17] A. N. Dey, *Thin Solid Films* **43** (1977) 131.
- [18] A. Streitwieser, Jr., 'Molecular Orbital Theory for Organic Chemists', John Wiley & Sons, New York (1961) p. 127.